INVESTIGATING THE SUBSURFACE STRUCTURE OF THE CHESNUT HILL EARTH EMBANKMENT DAM USING GRAVITY MEASUREMENTS

Ilan Valencius

Boston College

Department of Earth and Environmental Sciences

EESC6624: Environmental Geophysics

December 2023

Abstract

Information of the subsurface structure of the Chestnut Hill Reservoir earth embankment dam is needed to evaluate the long-term integrity of the dam for water storage and flood prevention. Finished in 1870, technical specifications of the dam are sparse yet vitally important as the dam is located directly above a residential area. In this study, the gravity anomalies were determined along a transect profile on the top of the dam using a Lacoste-Romberg gravimeter. After drift and latitude corrections are applied the gravity values increase to the south. This provides insight into the materials and construction of the dam, which thins towards the south. Combined with seismic refraction measurements from Maniscalco (2023), we demonstrate that the physical parameters of legacy dams can be retroactively constrained using passive methods—providing insight into further management and hazard mitigation. Code and data for this project is freely available at https://github.com/ivalencius/gravity-of-chestnuts.

Purpose of Work

Earth embankments levees and dams provide vital services across the US. From water storage to flood control, dams help protect both ecosystems and built infrastructure. For this reason, the structural integrity of dams is of the utmost importance to management agencies such as the US Army Corps of Engineers. Unfortunately, changing climactic conditions necessitate the reanalysis of many dams to ensure their safe and reliable operation.

Dam safety assessments have typically been performed using naïve estimations of future hydrology and other physical considerations such as earthquakes (Baecher, 2016) . Recent studies have shown that this approach is not suitable for the coming decades as future climactic conditions will exceed reasonable estimations derived from historical data – particularly in precipitation estimates (Hossain et al., 2010; Fluixá-Sanmartín et al., 2018). With these considerations in mind, many countries – such as Korea – are developing/improving existing dam safety regulations, instrumentation, and forecasting (Jeon et al., 2009).

A key component of dam and levee hazard assessment is the physical structure of the dam. Certain properties – such as dam height – may be easily monitored using conventional surveying equipment or other remote sensing approaches. Knowledge about the fill material and structure in embankment dams is much harder to constrain without detailed knowledge of the construction. In New England, there are about 400 high hazard potential dams constructed before the turn of the century (*Figure 1*). High hazard potential dams are expected to cause loss of human life if they were to fail (Arsenault). One such dam – the Chestnut Hill Reservoir dam – was finished in 1870 and serves as case study for managing these legacy dams. Sitting above a residential area, failure of the dam would lead to loss of human life. Information about the construction of the dam is sparse, with no information regarding the fill material or various other vital physical constraints. To close this knowledge gap, seismic methods may be used to infer subsurface parameters of the dam (Maniscalco, 2023). Other

geophysical methods may also prove useful. For this study, the bedrock structure of the Chestnut Hill Reservoir Dam is determined using gravimeter measurements.

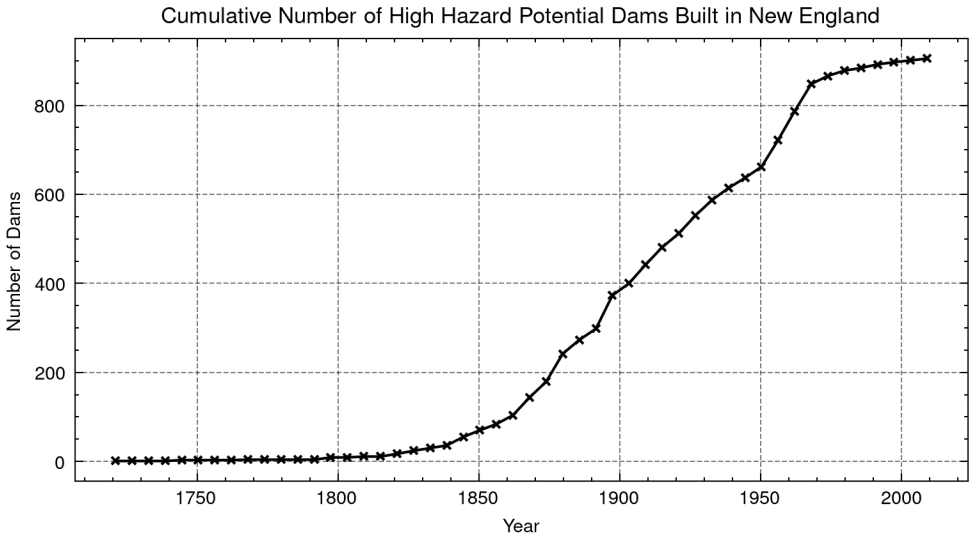

Figure 1. *The cumulative number of high hazard potential dams built in New England from the National Inventory of dams (US Army Corps of Engineers: Federal Emergency Management).*

Methods

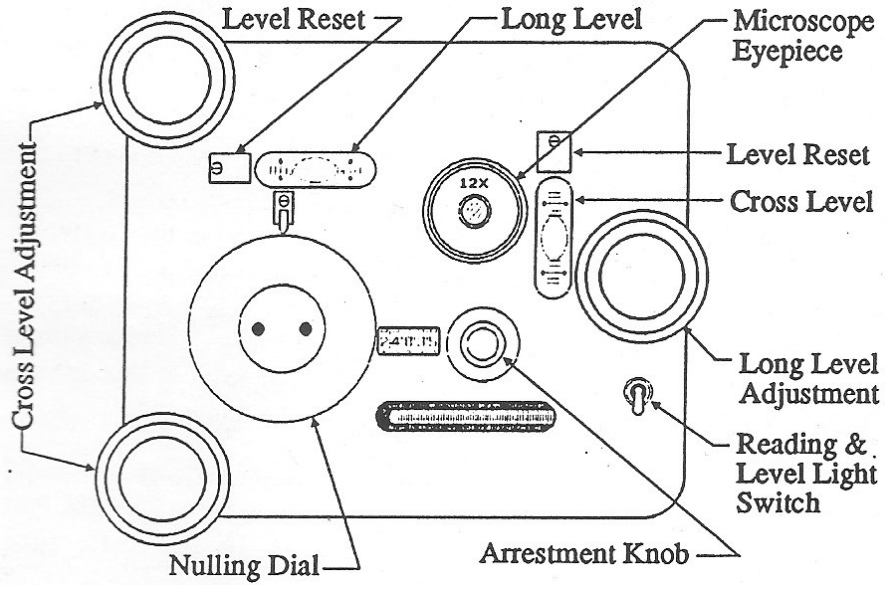

Figure 2. *Schematic of the LaCoste Romberg Gravimeter (Gravity Meters, Inc.).*

For this study, a LaCoste Romberg Model-G gravimeter was used (*Figure 2*). The fundamental theory behind using a gravimeter is the determination of gravitational variation due to changes in density in the subsurface (Kearey et al., 2011). For a point of mass m, the gravitational attraction at a radius r is given by:

$$\Delta g_r = \frac{Gm}{r^2} \text{ (eq. 1)}$$

As the LaCoste Romberg gravimeter only measures the vertical gravitational component, we modify eq. 1 so it becomes:

$$\Delta g_z = \frac{Gm}{r^3} \text{ (eq. 2)}$$

The value of interest is the relative gravitation anomaly relative to some reference point p_0. For this study p_0 is the start of the study transect, the most northward sampling location. The relative anomaly at each sampling location i is thus:

$$\Delta g_{z_i} = \Delta g_i - \Delta g_{p_0} \text{ (eq. 3)}$$

To correct for solid-earth tides, multiple measurements must be made at the same location to infer background changes to the gravity of the sample region over time. A linear correction can be used to retroactively correct all data collected between base-station samples (Kearey et al., 2011). This is known as a the “drift correction”. A

number of other corrections can also be applied, but since the surface of the dam is level, only a latitude correction is required.

The radius of the earth is smaller at the poles, decreasing r. This leads to higher values of gravity as you go north. To implement the latitude correction, we approximate our study as a N-S transect. Due to the small amount of zonal movement, this is a reasonable approximation. At each sample location, we determine the latitudinal gravity anomaly using:

$$g_{L_i} = 978031.85(1 + 0.005278897 \sin^2\left(\theta_0 - \frac{x}{111{,}111\ m}\right) + 2.3462 * 10^{-5} \sin^4\left(\theta_0 - \frac{x}{111{,}111\ m}\right) \quad \text{(eq. 4)}$$

Where x is the distance south along the transect in meters and θ_0 is the reference latitude of our starting point. Eq. 4 uses the conversion that 1 degree of latitude at 45° N is equal to 111,111 m. Boston is located at roughly 42° N so this is a valid approximation. We then correct every latitude measurement by compensating for the difference relative to the starting sample location:

$$\Delta g_{L_i} = g_{p_0} - g_{L_i} \quad \text{(eq. 5)}$$

Once the corrected gravitational anomaly data is determined, we can attempt to match the profile using numerical modeling. We can construct a 3-D grid with a theorized density profile. For a small enough grid size, we can approximate each square grid cell as a circle, allowing us to use eq. 2 for a point mass through Newton's Shell theorem which states that a spherically symmetric object acts as a gravitation point mass.

Experimental Data

On November 12, 2023, 37 gravimeter measurements were taken on top of the dam at 20 m spacing. See *Figure 3* for a visualization of sampling locations. Samples were taken starting at 42.33762° N, 71.15458° W then south along the water side of the dam every 20 m. The first base station – valid from 13:34 to 14:37 h – was the start of the transect. To minimize travel time, a second base-station was then established on the southmost block of the northern pumphouse. This base-station was used from 14:41 till the end of the study. The measurement data is shown in Table 1 (Note: Values of time are given in [24h time of day].[minutes/60] in order to facilitate an easier drift correction.)

Figure 3. *Map of gravimetry sampling stations starting at 42.33762° N, 71.15458° W. The triangle at each sample location points in the direction of the transect. Inset map*

shows the location of Chestnut Hill Reservoir relative to Boston. An 1899 image of the northmost pumphouse (used as base station 2) is shown in the bottom right (Hildreth, 1899).

Data Analysis

Table 2 displays the resulting anomaly data after applying the necessary interval factor and latitude corrections as well as the intermediate steps. The anomaly along the profile is shown in *Figure 4*. There is one large deviation from the apparent linear trend which occurs at roughly 400 m.

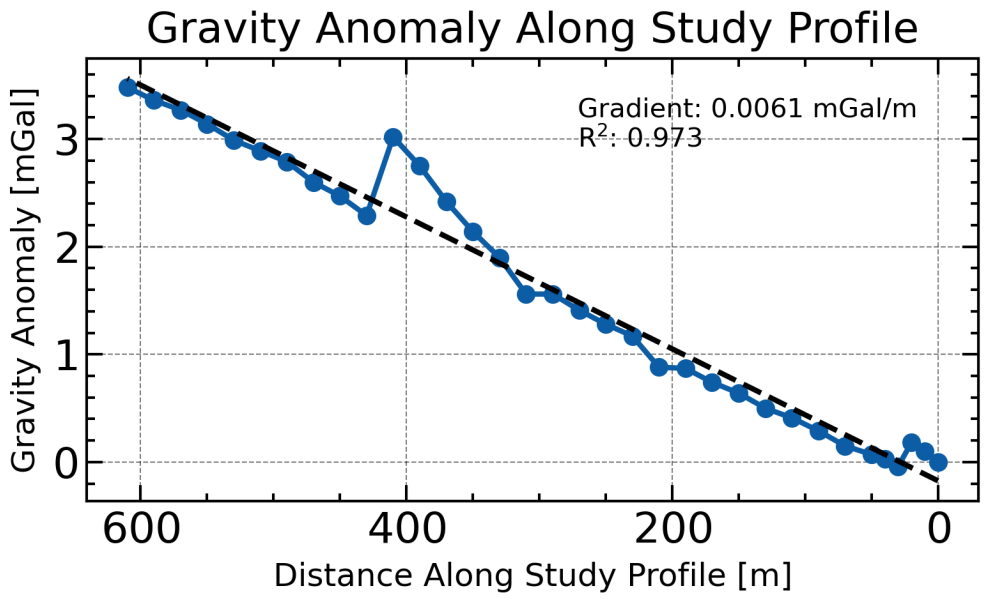

Figure 4. *Determined gravity anomaly on top of the Chestnut Hill Reservoir Dam. The study profile starts at the northmost sampling point and extends south.*

The model grid is 800x150x3 unit cells large (see *Table 3* for a more comprehensive overview of model parameters). Each unit cell is 1 m large. At each cell, we store an estimated density value. The bedrock under the Chestnut Hill Reservoir is part of the Roxbury Conglomerate unit with an estimated density of 2620 kg/m^3

(Ginsburg, 1959). From Maniscalco (2023), we can estimate depth to bedrock from seismic methods (*Figure 5)*. The bedrock can be estimated as northward dipping layer with slope 0.0159 m/m and an estimated depth of 12 m at the first gravimeter sampling location. A dipping plane with these parameters was then added to the model as the bedrock layer. Above this layer, the dam fill was added. The density of the dam fill material was estimated using data from Maniscalco (2023), Table 6. At his station 4, he estimated layer thicknesses and density from p and s-wave velocities. The estimated fill was calculated according to a density average weighted by layer thickness:

$$\frac{\left[\left(1\ m * 2000\frac{kg}{m^3}\right) + \left(0.2\ m * 2300\frac{kg}{m^3}\right) + \left(3\ m * 1000\frac{kg}{m^3}\right) + \left(3\ m * 1300\frac{kg}{m^3}\right)\right]}{7.2\ m} =$$

$$1300\ kg/m\text{^}3$$

This study assumes that this fill material is homogenous with respect to depth across the whole dam. In both the gravimeter data and the seismic data, a positive anomaly is observed at around 400 m (*Figure 4,5*). To mimic this, a 40 m by 3 m bedrock intrusion – density 2620 kg/m^3 – was added to the dam model at 4 m depth. Interpolating a dipping plane to a grid introduced sharp discontinuities between cells so the whole model was blurred using a gaussian filter with sigma=1 from the ‘scipy’ python library. The density model of the dam is shown in *Figure 6.*

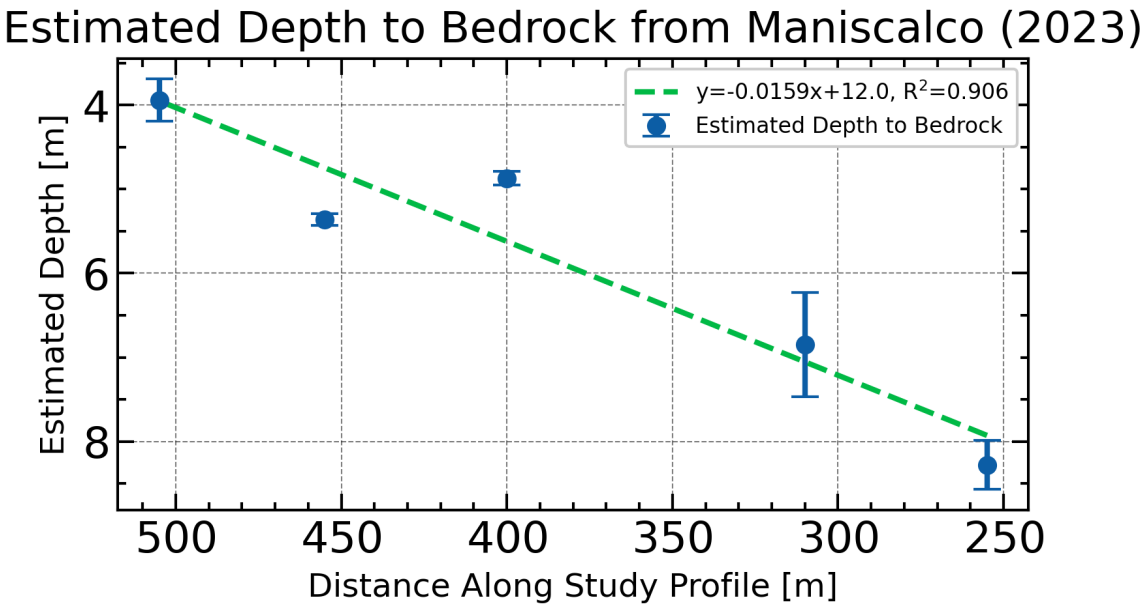

Figure 5. *Estimated depth to bedrock from seismic methods (Table 1 in Maniscalco, 2023).*

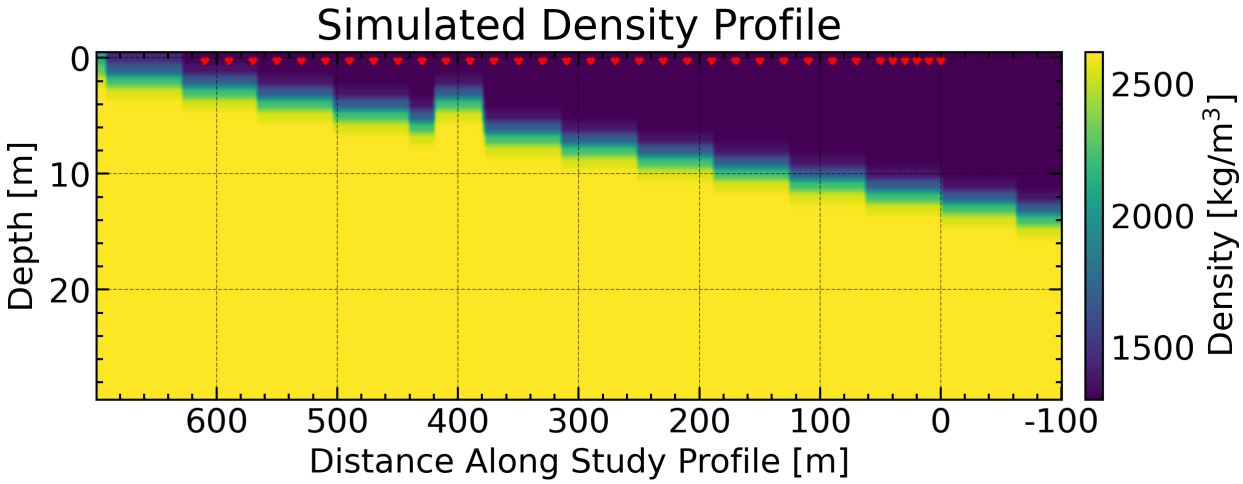

Figure 6. *Model profile of the dam sliced at y_size/2. Red triangles indicate the locations of gravimeter sampling with the start of the profile being the right-most triangle.*

Discussion

Figure 7 shows the results of the gravity modeling with gravity values being obtained at every location where gravimeter samples were taken (see *Figure 6*). The observed (black) and modeled (red) anomaly trends across the dam are similar in

shape, with a Pearson correlation coefficient of 0.981, which is significant at a p-value of 10^{-24}. A Pearson correlation coefficient of +1 indicates perfect linear fit. To match exactly, the densities in each cell were increased by a factor of 55 which yielded an anomaly trend that was equal in magnitude to the observed anomaly. This result indicates that the model scale was perhaps too small.

The model of the dam slightly overpredicts at the start of the profile and underpredicts at around 380 m. This is an indication that the slope of the bedrock is slightly too shallow, but it is a near match. The addition of the bedrock intrusion to the density model accurately represents the positive excursion found in both the gravimeter modeling and Maniscalco (2023). Significant overprediction near the end of the profile – 500+ m – is an indication that the bedrock is deeper then modeled at this section, although it appears to remain a dipping linear layer.

Further extensions of this study may include a larger grid size, as well as the integration of the dam morphology. This study approximated as a N-S profile, but the gravimeter measurements were taken on a slight curve. This means the apparent dipping layer may dip slightly east or west. From *Figure 5*, incorporating a variation in dip along the profile may further improve prediction, particularly at the end of the study profile.

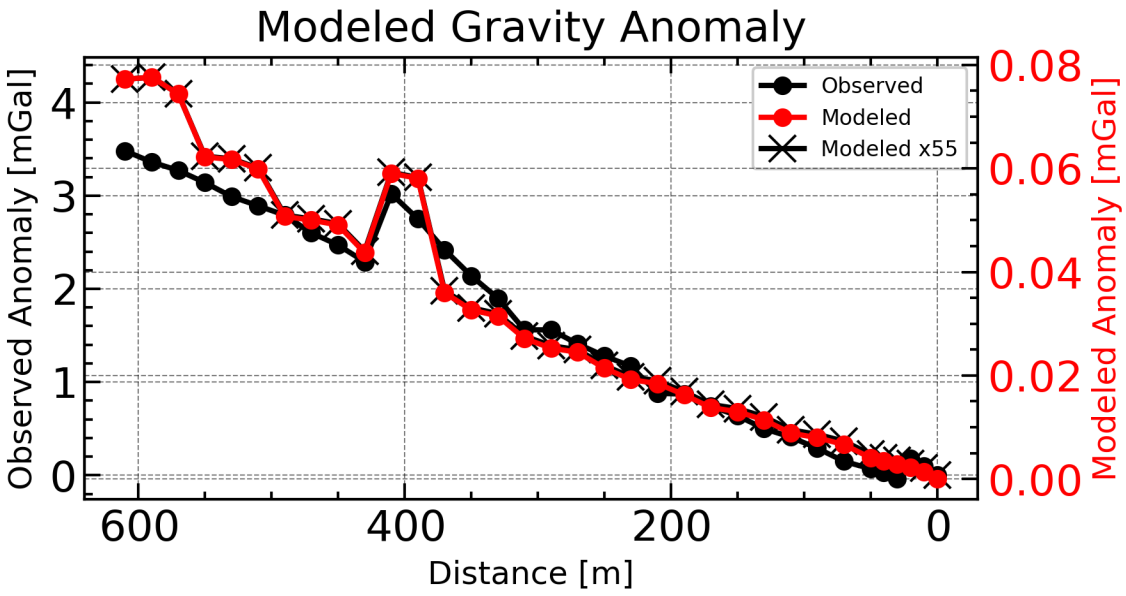

Figure 7. *Observed (black) and modelled (red) gravity anomalies across the dam model. Both the observed and modeled anomalies are the same shape but artificially increasing the model densities by a factor of 55 makes the modeled anomaly match the observed in scale (black crosses).*

References

Arsenault, F. Federal Guidelines for Dam Safety, Hazard Potential Classification System for Dams, April 2004:

Baecher, G.B., 2016, Uncertainty in dam safety risk analysis: Georisk: Assessment and Management of Risk for Engineered Systems and Geohazards, v. 10, p. 92–108, doi:10.1080/17499518.2015.1102293.

Fluixá-Sanmartín, J., Altarejos-García, L., Morales-Torres, A., and Escuder-Bueno, I., 2018, Review article: Climate change impacts on dam safety: Natural Hazards and Earth System Sciences, v. 18, p. 2471–2488, doi:10.5194/nhess-18-2471-2018.

Ginsburg, M., 1959, A Gravity Survey of the Boston Basin Region:

Gravity Meters, Inc. Instruction Manual for Lacoste & Romberg, Inc MODEL G and D GRAVITY METER:, https://www.aseg.org.au/sites/default/files/filefield_paths/Instruction%20Manual%20for%20Lacoste%20%26%20Romberg%2C%20Inc%20MODEL%20G%20and%20D%20GRAVITY%20METER.pdf.

Hildreth, J.L., 1899, Distribution Department, Chestnut Hill Reservoir, Effluent Gatehouse, Brighton, Mass., Apr. 14, 1899: Digital Commonwealth, https://www.digitalcommonwealth.org/search/commonwealth:qb98n177j.

Hossain, F., Jeyachandran, I., and Pielke, R., 2010, Dam safety effects due to human alteration of extreme precipitation: Water Resources Research, v. 46, p. 2009WR007704, doi:10.1029/2009WR007704.

Jeon, J., Lee, J., Shin, D., and Park, H., 2009, Development of dam safety management system: Advances in Engineering Software, v. 40, p. 554–563, doi:10.1016/j.advengsoft.2008.10.009.

Kearey, P., Brooks, M., and Hill, I., 2011, An introduction to geophysical exploration: Blackwell Publishing.

Maniscalco, S.J., 2023, USING THE HVSR, MASW, AND SEISMIC REFRACTION ANALYSIS METHODS TO ESTIMATE THE SUBSURFACE SEISMIC STRUCTURES OF TWO EARTH EMBANKMENT DAMS:

US Army Corps of Engineers: Federal Emergency Management, W., DC National Inventory of Dams:

Tables

Table 1. *Data collected on the Chestnut Hill Reservoir Dam on November 12, 2023. Cyan colored cells indicate samples used as base station 1 while green color cells indicate samples used as base station 2. Readings for the LaCoste Romberg are in measurement units because an interval factor must first be applied in order to convert the measurement units to mGal (Gravity Meters, Inc.). Values of time are given in [24h time of day].[minutes/60] in order to facilitate an easier drift correction.*

Distance From Starting Location [m]	Time [h]	Reading [units]
0	13.57	3920.11
10	13.73	3920.09
20	13.83	3920.07
30	13.97	3919.74
40	14.03	3919.72
50	14.10	3919.67
70	14.17	3919.59
90	14.22	3919.57

110	14.28	3919.53
130	14.33	3919.47
150	14.38	3919.45
170	14.43	3919.39
0	14.53	3919.82
190	14.62	3919.32
210	14.68	3919.17
230	14.75	3919.26
250	14.78	3919.2
270	14.83	3919.15
290	14.90	3919.11
310	14.95	3919.09
330	15.03	3919.05
350	15.13	3919.07
370	15.20	3919.15
390	15.25	3919.29
410	15.32	3919.36
210	15.47	3918.59
430	15.62	3918.47
450	15.68	3918.53
470	15.73	3918.54
490	15.78	3918.6
510	15.85	3918.59
530	15.90	3918.56
550	15.95	3918.59
570	16.00	3918.59
590	16.05	3918.56
610	16.10	3918.55
210	16.22	3918.96

Table 2. *Measured data with corrections applied. The color scheme is the same as Table 1. All readings were within the 3900-4000 interval range so an interval factor of 1.02118 was used to convert measurement reading into mGal (Gravity Meters, Inc.). The latitudinal gravitational anomaly at the start of the transect was found to be 983189.3447 mGal (using eq. 4 with a latitude of 42.33762° N).*

Distance From Starting Bench [m]	Time [h]	Reading [units]	Slope at Stations [units]	Drift Correction to t=0 [units]	Data corrected for drift [units]	Latitude Anomaly [mGal]	Interval Factor + Latitude Anomaly [mGal]	Anomaly Relative to Start [mGal]
0	13.57	3920.11		0.000	3920.11	0	4003.059528	0
10	13.73	3920.09		0.050	3920.14	0.06905644166	4003.159219	0.09969124166
20	13.83	3920.07		0.080	3920.15	0.138196332	4003.23857	0.179042732
30	13.97	3919.74		0.120	3919.86	0.2074196697	4003.011657	-0.04787033028
40	14.03	3919.72		0.140	3919.86	0.2767264519	4003.080964	0.02143645193
50	14.10	3919.67		0.160	3919.83	0.3461166768	4003.119719	0.06019187681
70	14.17	3919.59		0.180	3919.77	0.4851474441	4003.197481	0.1379530441
90	14.22	3919.57		0.195	3919.77	0.6245119537	4003.331739	0.2722117537
110	14.28	3919.53		0.215	3919.75	0.7642101871	4003.451014	0.3914867871
130	14.33	3919.47		0.230	3919.70	0.9042421262	4003.545094	0.4855665262
150	14.38	3919.45		0.245	3919.70	1.044607753	4003.680354	0.6208263526
170	14.43	3919.39		0.260	3919.65	1.185307048	4003.775101	0.7155734478
0	14.53	3919.82	-0.3	0.290	3920.11	0	4003.059528	0
190	14.62	3919.32	Include in above drift	0.315	3919.64	1.326339993	4003.900817	0.8412889933
210	14.68	3919.17		0.335	3919.51	1.46770657	4003.909432	0.8499047704
230	14.75	3919.26		0.384	3919.64	1.609406761	4004.193443	1.133915557

250	14.78	3919.2		0.409	3919.61	1.751440546	4004.29941	1.23988284
270	14.83	3919.15		0.446	3919.60	1.893807907	4004.428524	1.368996848
290	14.90	3919.11		0.495	3919.61	2.036508825	4004.580785	1.521257562
310	14.95	3919.09		0.532	3919.62	2.179543282	4004.741201	1.681673465
330	15.03	3919.05		0.594	3919.64	2.322911259	4004.90673	1.847202787
350	15.13	3919.07		0.668	3919.74	2.466612737	4005.146464	2.086936758
370	15.20	3919.15		0.718	3919.87	2.610647697	4005.422598	2.363070714
390	15.25	3919.29		0.755	3920.04	2.755016119	4005.747734	2.688206183
410	15.32	3919.36		0.804	3920.16	2.899717986	4006.014323	2.954795446
210	15.47	3918.59	-0.7404255319	0.915	3919.51	1.46770657	4003.909432	0.8499047704
430	15.62	3918.47		0.841	3919.31	3.044753279	4005.288374	2.228846439
450	15.68	3918.53		0.808	3919.34	3.190121977	4005.461428	2.40189992
470	15.73	3918.54		0.783	3919.32	3.335824063	4005.592153	2.532624992
490	15.78	3918.6		0.759	3919.36	3.481859516	4005.774269	2.714741432
510	15.85	3918.59		0.726	3919.32	3.628228319	4005.876841	2.817313817
530	15.90	3918.56		0.701	3919.26	3.774930451	4005.96772	2.908192535
550	15.95	3918.59		0.677	3919.27	3.921965893	4006.120202	3.060674164
570	16.00	3918.59		0.652	3919.24	4.069334626	4006.242382	3.182854284
590	16.05	3918.56		0.627	3919.19	4.217036631	4006.33426	3.274732876
610	16.10	3918.55		0.603	3919.15	4.365071889	4006.446896	3.38736792
210	16.22	3918.96	0.4933333333	0.545	3919.51	1.46770657	4003.909432	0.8499047704

Table 3. *Parameters used in model.*

Code Parameter	Value	Unit	Description
G	6.67430E-11	m^3/kg^1s^2	Gravitational constant.
GRID_SPACING	1	Meters	Spacing of grid cells (i.e. 1 unit cell = 1 m).
BUFFER	100	Unit cells	Buffer size of the model.
x_size	600+BUFFER*2	Unit cells	Size of along-dam dimension
y_size	50+BUFFER	Unit cells	Size of surface dimension perpendicular to the study profile.
z_size	30	Unit cells	Depth of model.
bedrock_density	2620	kg/m^3	Density of Roxbury Conglomerate (Ginsburg, 1959).
fill_density	1300	kg/m^3	Density of dam fill.